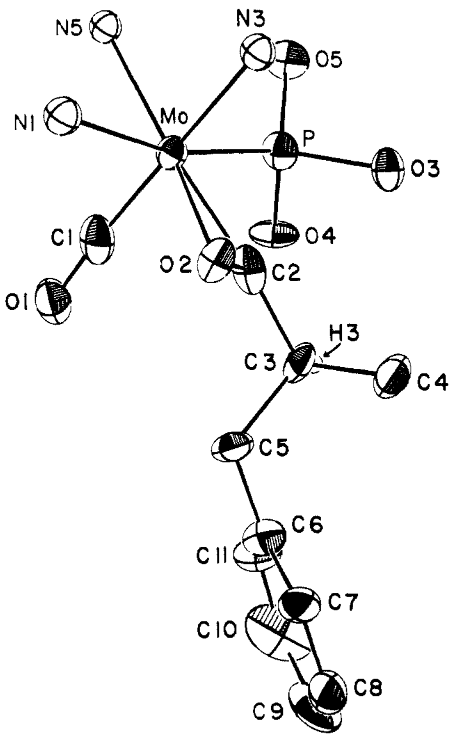

Figure 1. ORTEP diagram of the molybdenum coordination sphere in (Tp′)Mo(CO)[P(OPh)$_3$][η^2-C(O)CHMeBz] (**7a**) illustrating the atomic numbering scheme. Thermal ellipsoids are drawn at the 40% probability level.

was detected in the ^{31}P spectrum, suggesting greater than 98% diastereoselectivity. Confirmation that the alkylation reaction is kinetically controlled was obtained by generating the η^2-benzylated methyl acyl, η^2-C(O)CH$_2$CH$_2$Ph (**8**),[14] which was then deprotonated and allowed to react with MeI. Only **7b** was detected by ^{1}H NMR following chromatography. A crystal structure of **7a** has been undertaken;[15] the geometry shown in Figure 1 is very similar to previous η^2-acyl TpM(CO)L[C(O)R] structural reports.[6b,16]

Aldol condensation reactions of transition-metal enolates have not been reported as frequently as alkylation reactions.[17] We find that metal enolate **3b** reacts with benzaldehyde to yield a deep indigo η^2-enone derivative resulting from dehydration of the initial β-hydroxy η^2-acyl product. (Note that the molybdenum η^2-benzoyl complex which has been structurally characterized is also highly colored.[16a]) The formation of (Tp′)CO)$_2$Mo(η^2-C(O)CMe=CHPh) (**9**)[18] suggests that a range of electrophiles will react with these molybdenum(II) enolate reagents.

---

(14) **8**: IR(THF) 1816 cm^{-1} (ν(CO)); ^{1}H NMR (CD$_2$Cl$_2$) 3.2–4.7 (m, C(O)(CH_2)$_2$Ph).

(15) The crystal selected was triclinic of space group $P\bar{1}$ with unit cell dimensions $a = 14.142$ (4) Å, $b = 15.625$ (4) Å, $c = 11.147$ (2) Å, $\alpha = 99.88$ (2)°, $\beta = 92.23$ (2)°, $\gamma = 90.50$ (2)°, and $z = 2$. Data were collected with an Enraf-Nonius CAD4 diffractometer (Mo Kα radiation). Of the 4139 reflections monitored, 3017 reflections with $I > 3\sigma(I)$ were used in the structure solution. Final agreement indices of $R = 7.7\%$ and $R_w = 6.8\%$ resulted with hydrogens placed in calculated positions, the phenyl carbons of the triphenylphosphite and all of the hydridotris(3,5-dimethylpyrazolyl)borate atoms refined isotropically, and the remaining atoms refined anisotropically.

(16) (a) Desmond, T.; Lalor, F. J.; Ferguson, G.; Ruhl, B.; Parvez, M. *J. Chem. Soc., Chem. Commun.* **1983**, 55–56. (b) Curtis, M. D.; Shiu, K. G.; Butler, W. M. *J. Am. Chem. Soc.*, in press. (c) Molybdenum(II) η^2-acyl complexes which do not contain pyrazolyl borate ligands have also been prepared and structurally characterized; see: Carmona, E.; Sanchez, L.; Martin, J. M.; Proveda, M. L.; Atwood, J. L.; Priester, R. D.; Rogers, R. D. *J. Am. Chem. Soc.* **1984**, *106*, 3214–3222.

(17) (a) Liebeskind, L. S.; Welker, M. E. *Organometallics* **1983**, *2*, 194. (b) Davies, S. G.; Dordor-Hedgecock, I. M.; Warner, P. *Tetrahedron Lett.* **1985**, *26*, 2125. (c) Aktogu, N.; Felkin, H.; Baird, G. J.; Davies, S. G.; Watts, O. *J. Organomet. Chem.* **1984**, *262*, 49–58.

(18) **9**: IR (KBr) 1943, 1846 cm^{-1} (ν(CO)); ^{1}H NMR (CD$_2$Cl$_2$) δ 2.62 (d, $^3J_{HH} = 1.3$ Hz, C(CH$_3$)=, 7.46–7.73 (m, CHC$_6H_5$), 7.99 (q, $^3J_{HH} = 1.3$ Hz, =CHPh); ^{13}C{^{1}H} NMR (CD$_2$Cl$_2$) δ 130.0 (q, $^2J_{CH} = 8$ Hz, C(CH$_3$)=), 148.9 (dq, $^1J_{CH} = 159$, $^3J_{CH} = 4$ Hz, =CHPh), 238.5 (C(O)C(CH$_3$)).

Acknowledgment. Generous support of this research by the National Science Foundation (CHE-8310121) is gratefully acknowledged.

Supplementary Material Available: Tables of ^{1}H and ^{13}C NMR data for **2–9**, analytical data for **5**, **6**, and **7a**, X-ray data collection parameters for **7a**, and positional and thermal parameters and bond distances and angles for **7a** (21 pages). Ordering information is given on any current masthead page.

Hydrogenolysis of *n*-Butane over the (111) and (110)-(1×2) Surfaces of Iridium: A Direct Correlation between Catalytic Selectivity and Surface Structure[†]

J. R. Engstrom[‡] and D. W. Goodman*

Surface Science Division, Sandia National Laboratories
Albuquerque, New Mexico 87185

W. H. Weinberg*

Division of Chemistry and Chemical Engineering
California Institute of Technology
Pasadena, California 91125

Received March 24, 1986

The importance of surface structure in determining the activity and selectivity of various classes of heterogeneously catalyzed reactions is well-known. Boudart[1] has applied Taylor's concept of "active centers"[2] to catalysis by supported metals, stressing the need to examine the sensitivity of the *specific activity* (per site basis) to the average metallic particle size ("dispersion"). Although many reactions over supported catalysts, including the hydrogenolysis of alkanes, have been found to be "structure-sensitive",[1] a microscopic understanding of this variation in catalytic properties with particle size has remained elusive. Except in the limit of nearly atomic dispersion, changes in the surface of the catalyst particle with size will be geometric,[3] involving variations in the relative number of atoms in high-symmetry microfacets and at low-coordination-number edge and corner positions where these high-symmetry planes intersect.[5]

Foger and Anderson[6] have reported that the selectivity for the hydrogenolysis of n-C$_4$H$_{10}$ by supported Ir catalysts is extremely sensitive to the average metal particle size.[7] The structure sensitivity is most apparent for clusters of diameter $\lesssim$40 Å, where there is a rapid change in the average coordination number of the metal surface atoms.[11] Since the use of oriented single crystals as catalysts allows an *unambiguous* assessment of the effects of

---

[†] Work performed at Sandia National Laboratories and supported by the U.S. Department of Energy under Contract DE-AC04-76DP00789. We acknowledge the partial support of the Office of Basic Energy Sciences, Division of Chemical Science.

[‡] Visiting from the Division of Chemistry and Chemical Engineering, California Institute of Technology, Pasadena, CA 91125.

(1) Boudart, M. *Adv. Catal.* **1969**, *20*, 153.

(2) Taylor, H. S. *Proc. R. Soc. London, Ser. A* **1925**, *108*, 105.

(3) Any perturbation in the electronic properties will result from the differing *surface* geometries. Strong metal–support interactions are negligible for nonreducible oxides such as Al$_2$O$_3$ and SiO$_2$, whereas they may be significant for reducible oxides such as TiO$_2$.[4]

(4) See, e.g.: Foger, K. In *Catalysis—Science and Technology*; Anderson, J. R., Boudart, M., Eds.; Springer-Verlag: Berlin, 1984; Vol. 6, p 227 and references therein.

(5) van Hardeveld, R.; Hartog, F. *Adv. Catal.* **1972**, *22*, 75.

(6) Foger, K.; Anderson, J. R. *J. Catal.* **1979**, *59*, 325.

(7) Similar results have been reported for the hydrogenolysis of n-C$_4$H$_{10}$ by supported Pt[8] and the hydrogenolysis of n-C$_5$H$_{12}$ by supported Pt[9] and Rh.[10]

(8) (a) Leclercq, G.; Trochet, J.; Maurel, R. *C. R. Acad. Sci., Ser. C* **1973**, *276*, 1353. (b) Guczi, L.; Gudkov, B. S. *React. Kinet. Catal. Lett.* **1978**, *9*, 343.

(9) Brunelle, J.-P.; Sugier, A.; Le Page, J.-F. *J. Catal.* **1976**, *43*, 273.

(10) Yao, H. C.; Shelef, M. *J. Catal.* **1979**, *56*, 12. Yao, H. C.; Yu Yao, Y.-F.; Otto, K. *J. Catal.* **1979**, *56*, 21.

(11) Poltorak, O. M.; Boronin, V. S. *Russ. J. Phys. Chem.* **1966**, *40*, 1436.

0002-7863/86/1508-4653$01.50/0

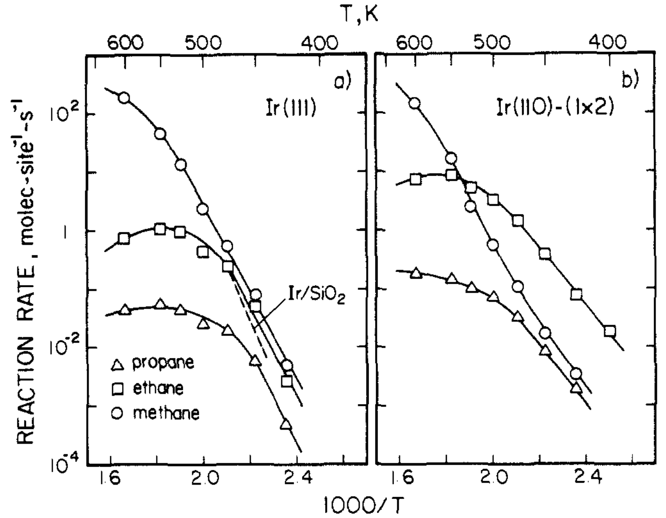

Figure 1. Specific reaction rates for the hydrogenolysis of n-C_4H_{10} over (a) an Ir(111) surface (n_s = 1.57 × 10^{15} sites cm^{-2}) and (b) and Ir(110)-(1×2) surface (n_s = 1.93 × 10^{15} sites cm^{-2}). The partial pressure of n-C_4H_{10} (>99.95% purity) is 1 torr, and that of H_2 (99.999% purity) is 100 torr. The dashed line in (a) represents data obtained by Foger and Anderson[6] over a 0.98 wt % Ir/SiO_2 catalyst ($\bar{d}_{Ir}$ = 70 Å; dispersion of 16%) extrapolated to our reactant partial pressures and plotted in terms of conversion. These data agree well with those for the Ir(111) surface.

surface geometry,[12] we have investigated the hydrogenolysis of n-C_4H_{10} over the close-packed (111) and the corrugated (110)-(1×2) surfaces of Ir. The clean Ir(110) surface is reconstructed into a (1×2) superstructure,[13] which contains a large fraction (25%) of low-coordination-number ($C_7{}^5$) edge atoms, whereas a perfect (111) surface contains no such atoms. If the ratio of the number of edge atoms to the number of face atoms influences the mechanism of this reaction, the (110)-(1×2) and (111) surfaces should be decisive in quantifying the connection between catalytic selectivity and *local* surface structure.

The experiments were performed in a high-pressure reaction chamber linked to an ultrahigh vacuum (UHV) analysis chamber in which facilities are available for Auger electron spectroscopy (AES) and ion sputtering.[12] The crystals were cleaned in the UHV chamber by Ar^+ sputtering, heating in 5 × 10^{-7} torr of O_2 at 700 K, and annealing to 1600 K. Reaction products were detected by gas chromatography.

Steady-state rates of the reaction of n-C_4H_{10} with H_2 for conversions below ~1% over both surfaces are shown in Figure 1, plotted in an Arrhenius form. Post-reaction surface characterization by AES indicated the presence of a *submonolayer* carbonaceous residue, the fractional coverage of which was nearly independent of reaction conditions; i.e., $\theta_c \cong 0.34 \pm 0.08$ on Ir(111) and $\theta_c \cong 0.24 \pm 0.08$ on Ir(110)-(1×2).[14] The only reaction products observed were CH_4, C_2H_6, and C_3H_8. The decrease in the apparent activation energy ("rollover") at $T \gtrsim 500$ K is associated with a depletion in the steady-state coverage of hydrogen.[12] Of more importance is the fact that the selectivities are quite different for the two surfaces where linear Arrhenius behavior is observed ($T \lesssim 475$ K). In this regime, the *major* reaction pathways are $n\text{-}C_4H_{10} + 2H_2 \rightarrow 2CH_4 + C_2H_6$ on Ir(111) and $n\text{-}C_4H_{10} + H_2 \rightarrow 2C_2H_6$ on Ir(110)-(1×2), with apparent activation energies of 34 ± 2 kcal mol^{-1} and 22 ± 2 kcal mol^{-1}. The profound difference in selectivity that is observed suggests that *different intermediates exist on the two surfaces.*

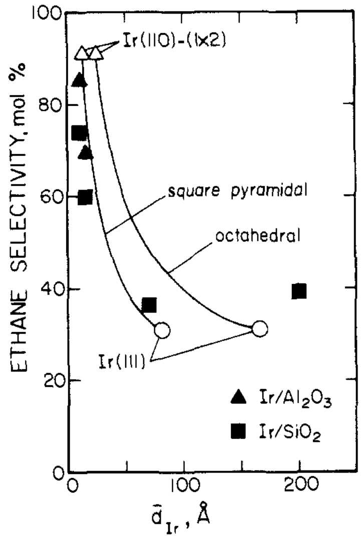

Figure 2. Selectivity for C_2H_6 production (mol % of total products) from the hydrogenolysis of n-C_4H_{10} over Ir catalysts plotted as a function of the mean Ir particle size. Data for the supported catalysts are from Foger and Anderson.[6] The abscissae for the two single-crystalline surfaces were determined by a calculated "effective particle size", as described in the text. The solid curves represent theoretical interpolations between the single-crystalline surfaces based on the specified geometrical shapes, as described in the text. The reaction temperature is in all cases ~475 K.

In order to compare the results of Foger and Anderson[6] to those reported here, we must compute an "effective particle size" for the (111) and (110)-(1×2) surfaces. *We shall introduce the ratio of the number of edge (C_7) atoms to the number of (111) face (C_9) atoms as the appropriate criterion of the "effective particle size".* The (110)-(1×2) surface contains one C_7 atom and two C_9 atoms per unit cell, a ratio of 1/2. The ratio for the (111) surface is determined both by defects and by the edge of the crystal (edge area/surface area $\lesssim$ 1/10). On the basis of hydrogen chemisorption data for this (111) surface,[16] the ratio C_7/C_9 is ~1/20. Assuming the supported catalyst particles form shapes of either octahedral or square-pyramidal (half-octahedral) structure,[17] the effective mean particle diameters are approximately 24 or 13 Å for the (110)-(1×2) surface, and 166 or 81 Å for the (111) surface, respectively.[18]

The selectivity for C_2H_6 production for both the supported catalysts[6] and the two single-crystalline surfaces are shown in Figure 2 as a function of the mean particle diameter.[19] Theoretically calculated curves, normalized to the specific activities of the two single-crystalline surfaces and interpolated by using the ratio C_7/C_9 as a basis, are also shown in Figure 2. Obviously, there is an *excellent* correlation between the selectivity for C_2H_6 production and the mean Ir particle size. Based on our results, *the observed increase in C_2H_6 selectivity with decreasing particle size is identified clearly with the increasing participation of low-coordination-number surface atoms.*

We have also observed that the specific rates (and selectivities) of hydrogenolysis of C_3H_8 over Ir(111) *and* Ir(110)-(1×2) and of n-C_4H_{10} over Ir(111) are virtually identical, with apparent activation energies of 34 ± 2 kcal mol^{-1}.[20] This implicates the presence of structurally similar, adsorbed intermediates in these

---

(12) Goodman, D. W.; Kelley, R. D.; Madey, T. E.; Yates, J. T., Jr. *J. Catal.* **1980**, *63*, 226. Goodman, D. W. *Acc. Chem. Res.* **1984**, *17*, 194.

(13) Chan, C.-M.; Van Hove, M. A.; Weinberg, W. H.; Williams, E. D. *Solid State Commun.* **1979**, *30*, 47. Chan, C.-M.; Van Hove, M. A.; Weinberg, W. H.; Williams, E. D. *Surf. Sci.* **1980**, *91*, 430.

(14) It has been shown previously that the (1×2) reconstruction of the Ir(110) surface is *not* removed by the presence of any coverage of hydrocarbon residues or surface carbon and hydrogen for temperatures between 100 and 800 K.[15]

(15) Weinberg, W. H. In *Surv. Prog. Chem.* **1983**, *10*, 1. Szuromi, P. D.; Weinberg, W. H. *Surf. Sci.* **1985**, *149*, 226.

(16) Engstrom, J. R.; Tsai, W.; Weinberg, W. H. manuscript in preparation. Szuromi, P. D.; Engstrom, J. R.; Weinberg, W. H. *J. Chem. Phys.* **1984**, *80*, 508.

(17) See, e.g.: Burch, R. In *Catalysis* (*Specialist Periodical Reports*); Bond, G. C., Webb, G., Eds.; The Royal Society of Chemistry: London, 1985; Vol. 8, p 149 and references therein.

(18) These two geometrical shapes will bracket other probable regular polyhedra, e.g., cubo-octahedra or cubes.

(19) Note that for the reaction $n\text{-}C_4H_{10} + H_2 \rightarrow 2C_2H_6$, the selectivity for ethane is 100%; whereas for the reaction $n\text{-}C_4H_{10} + 2H_2 \rightarrow 2CH_4 + C_2H_6$, the selectivity for ethane is 33%.

(20) Engstrom, J. R.; Goodman, D. W.; Weinberg, W. H., manuscript in preparation.

reactions. For n-C_4H_{10} hydrogenolysis over Ir(110)-(1×2), however, both the specific rate (apparent activation energy of 22 ± 2 kcal mol^{-1}) and the selectivity (to C_2H_6) are qualitatively different, indicative of the presence of a qualitatively different surface intermediate. Furthermore, by varying the partial pressures of the reactants, we have observed that *whatever* the intermediate from n-C_4H_{10} on Ir(110)-(1×2) is, it is *less dehydrogenated* than either the intermediate from n-C_4H_{10} on Ir(111) or the intermediate from C_3H_8 on both surfaces.[20] These observations suggest *strongly* that the occurrence of this particular intermediate on Ir(110)-(1×2) is a consequence of the corrugation of this surface rather than, for example, the presence of a particular, disordered carbonaceous residue on the surface. A very plausible intermediate in n-C_4H_{10} hydrogenolysis over Ir(110)-(1×2) is a metallacycle pentane. For example, it is known that transition-metal homogeneous complexes containing metallacycle pentane ligands can decompose thermally to two C_2H_4 ligands,[21] which would be hydrogenated to C_2H_6 under our experimental conditions, in agreement with the observed selectivity. The corollary to this hypothesis is that metallacycle pentane formation is favored on those surfaces that contain low-coordination-number metal atoms, and which is *necessary* from a stereochemical point of view on the two single-crystalline surfaces discussed here.

To summarize, the selectivity for C_2H_6 production from the hydrogenolysis of n-C_4H_{10} over Ir catalysts scales with the concentration of low-coordination-number metal surface atoms. This observation and detailed interpretation are limited neither to n-C_4H_{10} nor to Ir, however. Rather, they serve to illustrate the profound importance of local surface structure in dictating the occurrence of particular reaction intermediates and, hence, catalytic *selectivity.*

Registry No. Ir, 7439-88-5; butane, 106-97-8.

---

[21] (a) Grubbs, R. H.; Miyashita, A. *J. Am. Chem. Soc.* **1978**, *100*, 1300. Grubbs, R. H.; Miyashita, A.; Liu, M.; Burk, P. *J. Am. Chem. Soc.* **1978**, *100*, 2418. (b) Diversi, P.; Ingrosso, G.; Lucherni, A. *J. Chem. Soc., Chem. Commun.* **1977**, *52*. (c) McLain, S. J.; Wood, C. D.; Schrock, R. R. *J. Am. Chem. Soc.* **1977**, *99*, 3519. (d) McDermott, J. X.; Wilson, M. E.; Whitesides, G. M. *J. Am. Chem. Soc.* **1976**, *98*, 6529. (e) Harvie, I. J.; McQuillin, F. J. *J. Chem. Soc., Chem. Commun.* **1974**, 806. (f) Cassar, L.; Eaton, P. E.; Halpern, J. *J. Am. Chem. Soc.* **1970**, *92*, 3515. (g) Jacobson, D. B.; Freiser, B. S. *J. Am. Chem. Soc.* **1983**, *105*, 7492. (h) Armentrout, P. B.; Beauchamp, J. L. *J. Am. Chem. Soc.* **1981**, *103*, 6628.

Intramolecular [6 + 4] and [4 + 2] Tropone-Olefin Cycloaddition Reactions. Facile Synthesis of the Ingenane Ring System

Raymond L. Funk*[†] and Gary L. Bolton

Department of Chemistry, University of Nebraska—Lincoln
Lincoln, Nebraska 68588-0304

Received August 21, 1985
Revised Manuscript Received May 7, 1986

The intermolecular [6 + 4] and [4 + 2] cycloaddition reactions of tropone with dienes and monoenes, respectively, have been extensively examined[1] and exploited in recent synthetic endeavors.[2] Surprisingly, there has not been an investigation of the intramolecular variant of these reactions[3] which should be subject to the same rate acceleration and enforcement of regiospecificity observed in related intramolecular cycloaddition processes. An additional stimulus for this study is illustrated in Scheme I. Namely, the cyclization of appropriately functionalized 2-alkenyltropones should provide rapid access to the carbocyclic frameworks of the tumor promoter ingenol[4] (3), via an intra-

Table I. Cyclizations of 2-Alkenyltropones

2-Alkenyltropone	Cycloadduct	Conditions	Yield %[a]
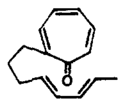 **7**	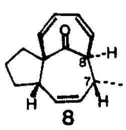 **8**	150°/36 h	88
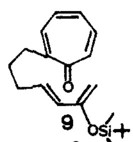 **9**	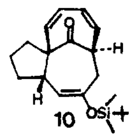 **10**	80°/6 h	92
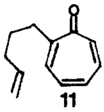 **11**	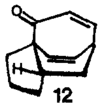 **12**	150°/36 h	81
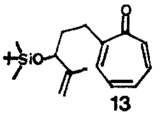 **13**	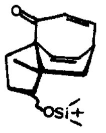 **14a** αOR **14b** βOR	200°/60 h 3.1 **14a**:**14b**	86
		0.1 eq. Et_2AlCl 110°/36 h >20:1	79
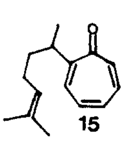 **15**	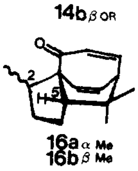 **16a** α Me **16b** β Me	240°/72 h 5:1 **16a**:**16b**	85
		0.1 eq. Et_2AlCl 110°/36 h 6.1	88
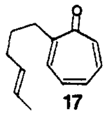 **17**	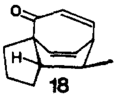 **18**	0.1 eq. Et_2AlCl 110°/30 h	80
		200°/72 h	77
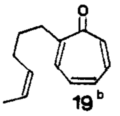 **19**[b]	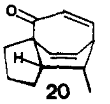 **20**	0.1 eq. Et_2AlCl 110°/12 h	78[c]
		150°/50 h	82[d]
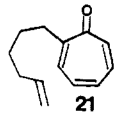 **21**	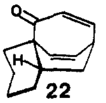 **22**	180°/60 h	85[e]
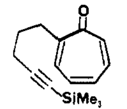 **23**	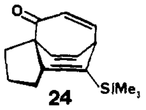 **24**	150°/96 h	67

[a] All new compounds reported herein exhibited satisfactory spectral (IR, NMR), analytical, and/or high-resolution mass spectral characteristics. [b] Contaminated by ~10% tropone **17** (^{13}C NMR analysis). [c] Yield based on recovered starting material (4%) and product contaminated with **18** (6%, ^1H NMR analysis). [d] Yield based on recovered starting materials (10%) and product contaminated with **18** (3%, ^1H NMR analysis). [e] Yield based on recovered **21** (42%).

[†] Fellow of the Alfred P. Sloan Foundation, 1985–1987.

[1] For a review, see: (a) Pietra, F. *Chem. Rev.* **1973**, *73*, 293. For recent investigations and leading references, see: (b) Uyehara, T.; Kitahara, Y. *Bull. Soc. Chem. Jpn.* **1979**, *52*, 3355. (c) Garst, M. E.; Roberts, V. A.; Houk, K. N.; Rondan, N. G. *J. Am. Chem. Soc.* **1984**, *106*, 3882. (d) Garst, M. E.; Roberts, V. A.; Prussin, C. *Tetrahedron* **1983**, *39*, 581.

[2] (a) Rigby, J. H.; Sage, J-M.; Raggon, J. *J. Org. Chem.* **1982**, *47*, 4815. (b) Uyehara, T.; Ogata, K.; Yamada, J.; Kato, T. *J. Chem. Soc., Chem. Comm.* **1983**, 17. (c) Garst, M. E.; Roberts, V. A.; Prussin, C. *J. Org. Chem.* **1982**, *47*, 3969.

[3] While this manuscript was in preparation, two examples of intramolecular tropone–olefin cyclizations surfaced. (a) An intramolecular [6 + 4] cycloaddition: Rigby, J. H., personal communication. (b) An intramolecular [6 + 2] photocycloaddition of an alkenyl tropone: Feldman, K. S.; Come, J. H.; Kosmider, B. J.; Smith, C. M. *Abstracts of Papers*, 190th National Meeting of the American Chemical Society, Chicago, IL; American Chemical Society: Washington, DC, 1985; ORGN 204.

0002-7863/86/1508-4655$01.50/0